Infrared Astronomy

The infrared part of the electromagnetic spectrum covers the wavelength range from about 1 mm (300 GHz) to 1 μm (300 THz). The infrared (IR) band is usually subdivided into the sub-millimeter (1 mm to 0.3 mm), the far- (0.3 mm to 50 μm, FIR), mid- (50 μm to 10 μm, MIR) and near-infrared (10 μm to 1 μm, NIR). At the long-wavelength end it connects to the radio domain and at the short end to the optical. In the FIR and most of the MIR domain astronomical sources cannot be observed from the ground. The other domains exhibit atmospheric windows of varying depth. Astronomical sources observed in the IR exhibit radiation temperatures of a few thousand to a few degrees kelvin. The most prominent sources are PLANETS, late-type stars, interstellar dust and gas clouds (see INTERSTELLAR MATTER), infrared luminous galaxies, the 3 K COSMIC MICROWAVE BACKGROUND and non-thermal extragalactic radio sources (QUASARS). Important reasons to carry out observations in the infrared are that the effect of dust extinction is minimized in this wavelength domain, the determination of the total luminosity of dust-enshrouded objects, and the fact that the visible to ultraviolet spectra of highly redshifted galaxies and quasars are shifted into the infrared while these objects become unaccessible in the optical due to extinction by hydrogen below a rest wavelength of 91 nm.

History

In 1800 Sir John HERSCHEL dispersed solar light through a glass prism onto several thermometers. Thomas Edison observed a total solar eclipse in 1878 in the infrared. In the early 1900s the Moon, planets and bright stars were observed in the infrared by S Pettit and E Nicholson. This work was continued by the systematic and extensive infrared studies of planets and stars by G KUIPER and H L JOHNSON in the 1950s (see Low and Rieke 1974). Frank J Low fully opened the field to astronomy in the early 1960s by inventing a low-noise gallium-doped germanium bolometer. In the following years the development of array detectors based on InSb and HgCdTe (up to 1024 $\times$ 1024 pixels) as radiation-sensitive substances determined the progress in the near-infrared. Balloon, airborne and satellite based observatories allowed measurements even at far-infrared wavelengths. Dedicated telescopes and sensitive bolometers and heterodyne receivers based on Schottky and SIS diodes opened the submillimeter domain.

Telescopes and observational techniques

The short NIR domain is contaminated by variable non-thermal atmospheric line emissions and with the exception of the NIR shortward of 2 μm the infrared is dominated by the thermal emission of the local background that includes the partially transparent atmosphere and all optical elements at the ambient temperature. Sensitive measurements are only possible from high mountains, balloons, airplanes or satellites using cooled instruments, detectors or (in space) even cooled telescopes. To further suppress the thermal background, secondary telescope mirror sizes are kept as small as possible and in the MIR the solid angle on the sky that is encompassed by individual detector elements is minimized in order to suppress the atmospheric thermal radiation. A novel technique in the short NIR is 'OH background suppression' which involves instrumental blanking of the OH line emission at a high spectral resolution. Stable background suppressed observations include observational techniques such as 'nodding' (measurements at alternating positions by moving the telescope back and forth) and 'chopping' (measurements at alternating positions by moving, for example, the secondary mirror at a frequency $\geq$1 Hz). The flux calibration is usually performed via a comparison with local radiation sources (black-bodies) at ambient ($\sim$300 K) or liquid nitrogen ($\sim$77 K) temperature or astronomical standards like planets, quasars or reference stars.

Usually the angular resolution of an optical/infrared telescope is limited to about one arcsecond due to the turbulent atmosphere. In order to obtain diffraction-limited images from the ground at several telescopes 'adaptive optics' has been employed (Alloin and Mariotti 1994, Tyson 1991). Traveling through the Earth's atmosphere the initially plane wave front from the object is distorted and measured at the telescope in the optical with a Shack–Hartmann or curvature wavefront sensor (see Tyson 1991). This signal is then used to control a deformable mirror that can correct the wavefront distortions in the NIR. The resulting images have a diffraction-limited part that contains typically up to 60% of the light. The angular resolution A in arcseconds that can be achieved depends on the observing wavelength λ in micrometers and the diameter D of the telescope in meters and can be calculated via $A(\text{arcsec}) \sim 0.206 \times \lambda/D$. For an 8 m class telescope it is of the order of 0.06 arcseconds at a wavelength of 2.2 μm. Combining different telescopes interferometrically subarcsecond angular resolutions can be obtained in the submillimeter domain (Downes 1989, Watt and Webster 1990). Interferometric measurements can also be applied in the MIR and NIR domain. They provide high-accuracy astrometry and information on stellar diameters and orbital elements of multiple stars.

Telescopes

A large amount of information has been gained with INFRARED TELESCOPES in the 2 to 4 m class (e.g. the Infrared Telescope Facility, IRTF, of NASA or the New Technology Telescope, NTT, of the EUROPEAN SOUTHERN OBSERVATORY, ESO). Large-aperture telescopes with dedicated NIR and MIR facilities are the Keck Telescope in Hawaii (10 m diameter) the ESO Very Large Telescope (VLT) on Paranal in Chile (four 8 m telescopes). Others like the LARGE BINOCULAR TELESCOPE (LBT; two mechanically coupled 8.4 m telescopes) at the MT GRAHAM INTERNATIONAL OBSERVATORY in Arizona, the multinational GEMINI OBSERVATORY twin 8.1 m telescopes in Chile and Hawaii, or the 8.3 m diameter

SUBARU TELESCOPE of Japan in Hawaii will soon come into operation. In addition to space missions that are summarized below, MIR and FIR observations have been carried out using the Kuiper Airborne Observatory (KAO) with a 36 in telescope on board a C-141 airplane at a height of up to about 14 km. This observatory will be followed by SOFIA (the USA/German Stratospheric Observatory for Infrared Astronomy), a 2.5 m mirror on board a Boeing 747. In the submillimeter domain large single-dish antennas like the NOBEYAMA RADIO OBSERVATORY 40 m dish in Japan and the 30 m telescope of IRAM (INSTITUT DE RADIO ASTRONOMIE MILLIMÉTRIQUE) in Europe and the JAMES CLERK MAXWELL TELESCOPE (JCMT) in Hawaii (15 m), as well as several millimeter wavelength interferometry arrays in the USA, Europe and Japan have contributed to the investigation of line and continuum emission of gas and dust in our own and external galaxies in the local universe and at cosmological redshifts. Further progress will be achieved in the near future via the infrared optimized NGST (Next Generation Space Telescope), interferometric arrays with a very large collecting area like the ALMA (the ATACAMA LARGE MILLIMETER ARRAY in northern Chile), as well as large bolometer and spectrometer focal plane array receivers for single dish telescopes.

Detectors

A broad variety of detector techniques is required in the infrared (e.g. Rieke 1994). In the NIR and MIR range large-format focal plane detector arrays are used. Arrays that use HgCdTe as IR sensitive material are hybrid structures. They have been built using molecular beam epitaxy and liquid phase epitaxy techniques to grow the infrared sensitive HgCdTe material. The spectral response for HgCdTe focal plane arrays typically used in astronomy ranges from from 0.8 μm to 2.4 μm. The backside illuminated material is connected to multiplexers of different formats (e.g. 1024×1024 pixels). For arrays that use InSb as a detector material the spectral response goes from 0.5 to 5.4 μm. Typical pixel sizes range between about 10 and 40 μm. About 60% to 80% of all incident photons are detected. Very low dark current and low read noise values make these arrays suited for long exposures under low-background conditions as realized in most astronomical applications. On the other hand, frame rates of above 10 Hz can be reached as well. A similarly high potential for low-background observations in the MIR have BIB (blocked impurity band) detectors.

Focal plane array detectors have also been used in the FIR. A 5×5 array of stressed Ge:Ga photoconductors was flown on the KAO in an imaging spectrometer. Such arrays have also successfully been operated in space (ISO-LWS and ISOPHOT, see below). Larger-format arrays will soon be used on SRTF (Space Infrared Telescope Facility) and FIRST (Far-Infrared and Submillimeter Telescope) and SOFIA. The wavelength range between approximately 80 and 210 μm can be covered with spectral resolutions ($R=\lambda/\Delta\lambda$) of the order of a few thousand.

In the submillimeter and FIR domain ^{3}He-cooled bolometers can be used to perform sensitive measurements of cold dust and faint continuum sources in general (e.g. SCUBA: Submillimetre Common-User Bolometer Array at the JCMT and the IRAM bolometer arrays). Heterodyne receivers for low-noise high-spectral-resolution measurements in the submillimeter range employ Schottky diodes (semiconductor–metal contacts) and SIS diodes (supraconductor/insulator/supraconductor tunneling contacts).

Physical mechanisms

The most prominent infrared continuum radiation mechanism in astrophysical sources is the BLACK-BODY RADIATION that follows a Planck law (see below). This radiation is emitted by all bodies, from dust to planets and stars, and peaks for temperatures below a few thousand kelvin in the infrared. For the ambient temperature of about 300 K the spectral peak is at a wavelength of 10 μm. Other important continuum radiation mechanisms are the free–free and synchrotron radiation emitted by thermal and relativistic plasmas respectively, in or near star-forming regions in our own galaxy and in the nuclei of Seyfert galaxies and quasars. The line emission is dominated by rotational lines in the millimeter and submillimeter domain, fine structure lines of atoms and ions in the FIR and rotational vibrational as well as recombination lines in the MIR and NIR domain. Due to large variations of optical depths and large column densities of emitting and absorbing material, radiative transport of energy is of special interest for both continuum and line radiation (e.g. Osterbrock 1974, Spitzer 1978).

Radiative transport

In a plane-parallel cloud, radiative transport at a frequency ν can be treated simply. The change of specific line intensity I_ν (erg s^{-1} cm^{-2} Hz^{-1} sr^{-1}) along an infinitesimal element dz along the line of sight through a molecular cloud is given by:

$$\frac{\mathrm{d}I_\nu}{\mathrm{d}z}=\frac{h\nu}{4\pi}n_u A_{ul}-\frac{h\nu}{4\pi}\Phi(\nu)I_\nu(n_u B_{ul}-n_l B_{lu})=\epsilon_\nu-\kappa_\nu I_\nu. \quad (1)$$

Here n_u, n_l are the volume densities of molecules in the upper and lower states of the transition, with the corresponding statistical weights g_u and g_l. The Einstein coefficient A_{ul} (s^{-1}) is the rate of decay of n_u by spontaneous radiative transitions. The line shape is described by $\Phi(\nu)$, normalized to $\int\Phi(\nu)\,\mathrm{d}\nu=1$. The volume emissivity and absorption coefficient are denoted by ϵ_ν and κ_ν. With these coefficients the sources function Σ_ν can be defined that is equivalent to Planck black-body radiation law and is the most important source function for electromagnetic radiation in the infrared:

$$\Sigma_\nu=\frac{\epsilon_\nu}{\kappa_\nu}=\frac{2h\nu^3}{c^2}\frac{1}{\exp(\frac{h\nu}{kT_{\mathrm{ex}}})-1}. \quad (2)$$

This gives the spectral energy density of a black-body as a function of the excitation temperature T_{ex}

(an equivalent Planck temperature) that describes the population of states l and u through a thermal Boltzmann population. Using Σ_ν and an optical depth through the cloud $\tau_\nu = -\int_0^z \kappa_\nu \, dz$ the radiative transport equation from above can be simplified to:

$$I_{\nu,\text{observed}} = I_{\nu,\text{background}} \, e^{-\tau_\nu} + \Sigma_\nu (1 - e^{-\tau_\nu}). \quad (3)$$

This equation shows that the absorption in a molecular cloud is proportional to $e^{-\tau_\nu}$ and the emission proportional to $(1 - e^{-\tau_\nu})$.

Line emission

Besides recombination lines of hydrogen and helium the IR exhibits a broad variety of fine structure lines from atoms and ions and rotational and vibrational lines of molecules. The line emission in the submillimeter and long-wavelength FIR is dominated by rotational transitions of simple diatomic and linear multiatomic molecules. They have a simple ladder of rotational energy states E_J depending on the rotational quantum number J and the rotational constant B(Hz) as (to first order):

$$E_J = hBJ(J+1). \quad (4)$$

Electric dipole transitions in molecules with permanent electric dipole moments occur at a frequency $\nu_J = 2BJ$. The maximum emission in the ladder populated at a temperature T_{rot} occurs approximately at $E_J = hBJ(J+1) \approx kT_{\text{rot}}$, or $J_{\max} \approx \sqrt{(kT_{\text{rot}})/(hB)}$. One of the most important molecules for millimeter and infrared astronomy is carbon monoxide (CO) with its lowest $J = 1$–0 rotational transition at 115 GHz (2.6 mm wavelength). In the submillimeter and FIR higher rotational transitions from warm (30 to 100 K) and hot (several 100 K) molecular gas can be observed. These transitions are excited via collisions of CO with H_2 molecules. The dipole line radiation of CO therefore indirectly traces the spatial distribution, density and temperature of molecular gas. Only a small fraction (in star-forming regions of entire galaxies typically one part in a million or less) of very hot molecular gas (a few 1000 K) can be observed via quadrupole radiation in ro(tational)-vibrational NIR lines from the H_2 molecule.

In case of ro-vibrational transitions of linear molecules that occur in the NIR domain the energy states are labeled by the vibrational (v) and rotational (J) quantum numbers

$$E(v, J) = \frac{h}{2\pi}\omega_0 \left(v + \frac{1}{2}\right) + hBJ(J+1). \quad (5)$$

The correction terms are due to centrifugal stretching and Coriolis coupling of the rotational and vibrational motions. The ro-vibrational lines in electric dipole transitions with $v \rightarrow v - 1$ and $J \rightarrow J \pm 1$ can be approximated via

$$\nu_{v,J\rightarrow J\pm1} = \omega_0 \pm 2hBJ(J+1). \quad (6)$$

An important band head of ro-vibrational CO line absorption is found in ~3000 K atmospheres of late-type stars in the NIR at a wavelength of 2.31 μm. It is used for instance to analyse stellar populations and kinematics in the nuclei of galaxies.

The line emission in the MIR and FIR is dominated by fine structure line transitions. In the optical thin limit the integrated line flux (erg s^{-1} cm^{-2}) of a fine structure line can be written as:

$$F_{\text{line}} = \frac{h\nu}{4\pi} \int_{\text{Beam}} \int_{\text{LOS}} n_u \, dl \, d\Omega. \quad (7)$$

Here LOS is the line of sight and $d\Omega$ the differential solid angle used to integrate the line emission over the telescope beam. An important fine structure line is the [CII] line at a wavelength of 158 μm. It is one of the brightest cooling lines of the interstellar medium and can contain up to almost 1% of the overall infrared luminosity of an entire galaxy. In figure 1 the infrared spectrum of the starburst galaxy M82 is shown.

Space missions

In the following some of the recent larger INFRARED SPACE MISSIONS are summarized briefly, both in terms of their technical definitions and scientific results.

IRAS

IRAS was launched on 25 January in 1983 with a telescope mounted in a liquid helium cooled cryostat. The telescope was a Ritchey–Chrétien design with a 0.57 m aperture. The mirrors were made of beryllium and cooled to approximately 4 K. During its 10 months of operation, and in addition to numerous pointed observations, IRAS surveyed more than 96% of the sky up to four times at four infrared bands centered at wavelengths of 12, 25, 60 and 100 μm with its detectors cooled to 3 K. The survey array consisted of 62 rectangular infrared detectors arranged in staggered rows such that any real point source crossing the focal plane as the satellite scanned the sky would be seen by at least two detectors in each wavelength band. The survey covered the sky in overlapping strips as the satellite was orbiting in its near-polar orbit, which precessed by about a degree each day. During some pointed observations, individual sources were mapped simultaneously at 50 and 100 μm using a cold internal chopper for flux reference. IRAS also contained a low-resolution spectrometer, which produced a relevant spectral atlas.

With 350 000 detected objects the IRAS mission increased the number of cataloged astronomical sources by almost 70% and has had a major impact on almost every area of astronomy. IRAS extended our knowledge on the evolution of external galaxies. The instruments on board the satellite detected ~75 000 starburst galaxies—galaxies which are extremely bright in the infrared due to their intense star formation. Many of these starburst galaxies showed signs of interaction with companion galaxies and have 'super winds' (galactic scale gaseous outflows) emerging from their centers due to the large number of supernova explosions which occur in these galaxies.

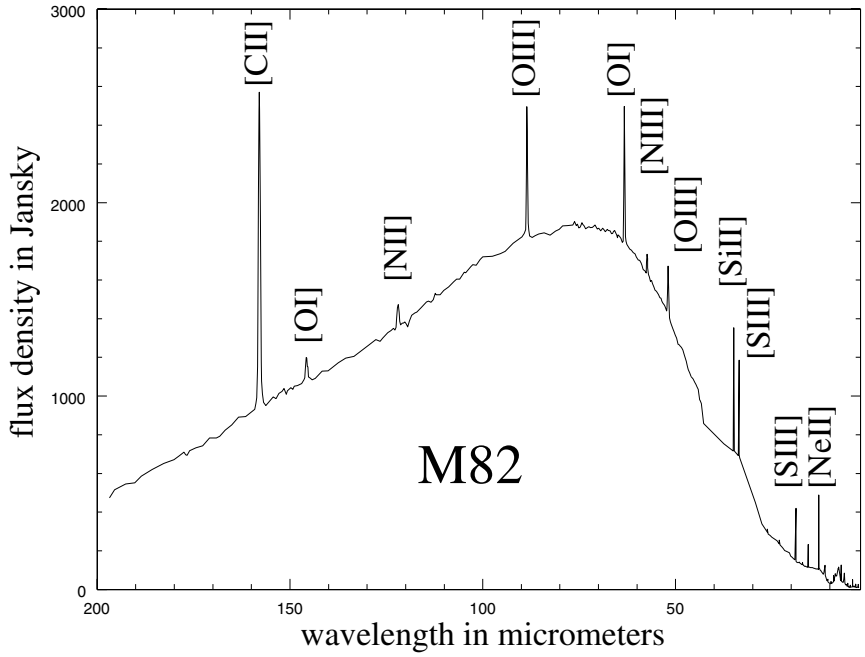

Figure 1. The infrared spectrum of the starburst galaxy M82 as taken with the ISO SWS and LWS spectrometer. In addition to the peak in the dust continuum emission, strong fine structure lines are indicated.

IRAS also found for the first time infrared cirrus: warm dust associated with diffuse clouds mostly at large galactic latitudes. IRAS discovered six new comets and found that comets in general are dustier than previously thought. The FIR observations provided evidence of zodiacal dust bands around other stars (e.g. Vega), and detected several probable protostars embedded in clouds of gas and dust.

ISO

The Infrared Space Observatory (ISO), (see figure 2) (Kessler *et al* 1996) of the European Space Agency (ESA) was an astronomical satellite, operating at wavelengths from 2.5–240 μm. Essentially, ISO consisted of a large cryostat which contained at launch about 2300 l of superfluid helium to maintain the Ritchey–Chrétien 60 cm diameter telescope, the scientific instruments and the optical baffles at temperatures of 2–8 K. ISO was launched by an Ariane 4 on 17 November 1995 and kept in operation for 29 months. The satellite spent roughly 16 h per day outside the radiation belts and during this time the sensitive FIR detectors could be operated. The four focal plane instruments on board ISO consisted of one short- and one long-wavelength spectrograph (SWS and LWS) and imaging experiments in the MIR (ISOCAM) and FIR (ISOPHOT) domain.

The SWS instrument consisted of two grating spectrometers, together covering the wavelength range between 2.38 and 45.2 μm. The overall spectral resolution covered a range of $R = 1000$ (300 km s^{-1}) to $R = 30\,000$ (10 km s^{-1}) by inserting Fabry–Pérot (FP) filters. In its grating mode, the LWS operated from 45 μm to 180 μm with a resolving power between a few 100 and 10 000 using FPs. The ISOCAM infrared imaging camera used

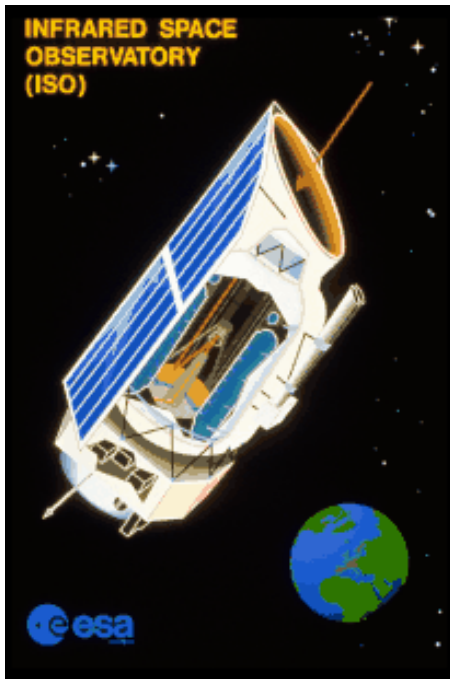

Figure 2. The Infrared Space Observatory.

two 32 × 32 pixel detectors, one devoted to the 2.5–5 μm range and the other to the 4–17 μm range. Images in direct and polarized light at several spatial resolutions through a variety of spectral filters could be taken. ISOPHOT was an imaging photopolarimeter for the wavelength range 2.5 to 240 μm and included a low-resolution spectrometer for the 2.5 to 12 μm range.

ISO observations resulted in the first measurements of the lowest rotational transition of molecular hydrogen H_2 at 28.1 μm which is important in determining the distribution and abundance of cold molecular material directly. ISOCAM observations determined the distribution of warm dust near star-formation regions in external galaxies. Via 200 μm imaging, ISO detected 5 to 10 times more 15 to 21 K cold dust than IRAS. LWS and SWS observations of luminous galaxies allowed the determination of the relative contribution of starburst and non-thermal activity in their nuclei.

COBE

The COBE satellite was developed by NASA's GODDARD SPACE FLIGHT CENTER to measure the diffuse infrared and microwave 2.7 K cosmic background radiation from the early universe (due to the Big Bang). It was launched on 18 November 1989 and carried three instruments, a far-infrared absolute spectrophotometer (FIRAS) to compare the spectrum of the microwave background with that of a black-body, a differential microwave radiometer (DMR) to map the cosmic radiation sensitively, and a diffuse infrared background experiment (DIRBE) to search for the cosmic infrared background radiation. The cosmic microwave background spectrum was measured with a precision of 0.005%; for the first time the background was found to have an intrinsic anisotropy, at a level of 1 part in 100 000. Absolute sky brightness maps from 1.25 μm to 240 μm were obtained and the background radiation was detected in the two longest DIRBE wavelength bands at 140 and 240 μm wavelengths.

NICMOS

NICMOS (near-infrared camera and multiobject spectrometer) was an instrument which has been installed in the HUBBLE SPACE TELESCOPE (HST) in orbit and allowed it to observe in the near-infrared. The camera was a second-generation Hubble instrument installed aboard the satellite during a servicing mission in February 1997. NICMOS provided the capability of both imaging and spectroscopy at wavelengths between 0.8 and 2.5 μm. NICMOS contained three cameras designed for simultaneous operation. The optics presented the detectors with three adjacent, but not spatially contiguous, fields of view of different image scales. NICMOS employ three low-noise, high-quantum-efficiency, HgCdTe 256 × 256 element focal plane arrays in a passive dewar using solid nitrogen as a coolant. The camera contained a variety of filters, grisms (a combination of a grid and a prism to allow for dispersion on the optical axis) and polarizers selected through three independent filter wheel mechanisms. Slitless imaging spectroscopy in the widest field camera provided a multiobject spectrographic capability with a resolution of ∼200. NICMOS achieved diffraction-limited performance at 1.0 and 1.75 μm.

Sensitive near-infrared images have been obtained of solar system planets, the central regions of nearby galaxies with ACTIVE GALACTIC NUCLEI (AGN)—like the nearest radio galaxy Centaurus A—or violent star formation activity as in Arp 220. NICMOS also provided a detailed stellar census of the stars in obscured or embedded star clusters like the ORION NEBULA and the galactic center. A comparison of long exposures taken toward selected regions of the so-called HUBBLE DEEP FIELD (HDF) allowed us to improve our knowledge on the spectral energy distribution of the most distant galaxies in the universe.

Sources

In general, dust-embedded sources or dense molecular clouds heated by stars or active galactic nuclei are most luminous in line and continuum radiation in the infrared. In galaxies the luminosity is concentrated toward the nuclei and some active star-forming regions mostly within spiral arms or in barred spirals at the tips of the bars. Ultraluminous galaxies belong to the most luminous objects in the universe and can exhibit more than 10^{12} (a million million) solar luminosities in the infrared. As typical examples of infrared bright objects the nuclear region of the Milky Way (the galactic center), ultraluminous galaxies and star-forming regions are discussed in the following.

Galactic center

Photospheric emission of stars in the galactic center at a distance of 8 kpc (26 400 light years; one parsec (1 pc) equals 3.3 light years) can only be observed in the near-infrared. The visible light from the central stellar cluster is obscured by about 30 magnitudes (one magnitude is a factor of 2.5 in intensity) due to the dust and gas in the galactic plane. High angular resolution, near-infrared imaging and spectroscopy have made it possible in the last few years to measure stellar proper motion and radial velocities in the galactic center down to separations of less than five light days from the compact radio source SgrA* (in the constellation Sagittarius) at the dynamic center of the Milky Way (Eckart and Genzel 1997, Genzel *et al* 1997, Ghez *et al* 1999). These measurements make a compelling case for the presence of a compact, central dark mass of 2.6×10^6 solar masses which is most likely in the form of a supermassive black hole.

The first indications for a central mass concentration in the Milky Way (for a summary see Genzel *et al* 1994) emerged in the late 1970s from spectroscopic observations of a mid-infrared fine-structure line of Ne^+. As radio interferometric observations had discovered a compact, non-thermal radio source, SgrA*, in the same region, a plausible interpretation—by analogy to quasars—was that the large gas velocities indicate orbital motions in the vicinity of a million solar mass black hole, coincident with SgrA*.

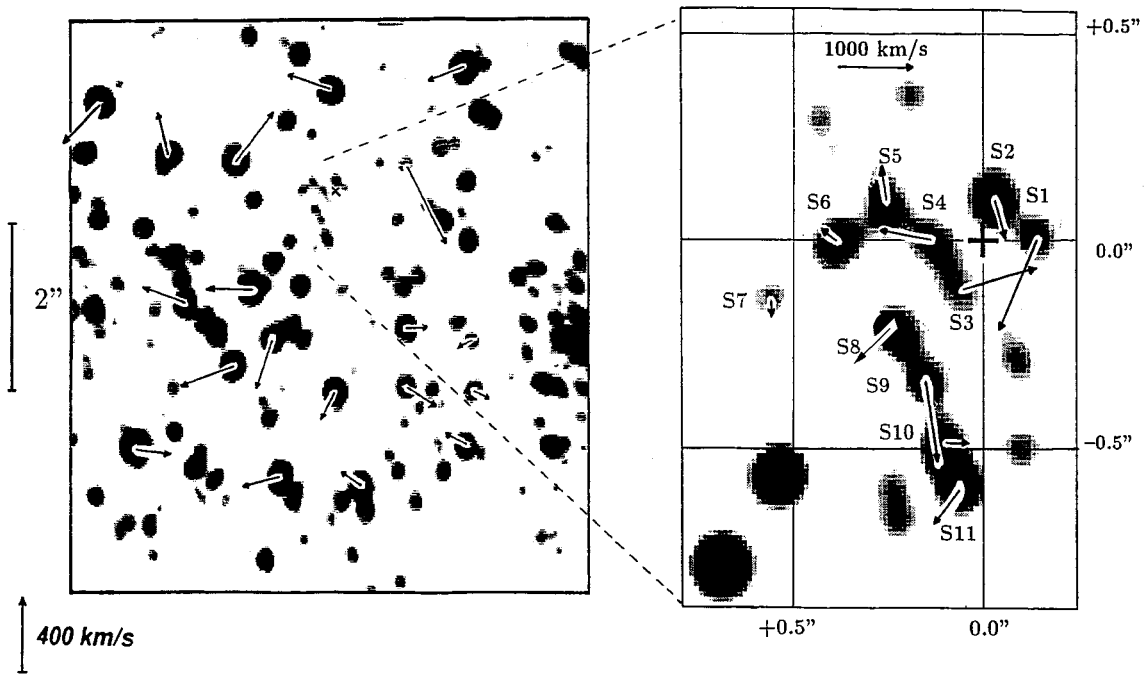

Figure 3. Proper motion vectors of the central sources close to Sgr A* at the galactic center.

In the following years further infrared (and radio) spectroscopic data including radial velocities of stars strengthened the gas dynamic evidence for a dark 1 to 3×10^6 $M_\odot$ central mass. Speckle interferometry revealed a compact 1″ diameter cluster of stars at the position of Sgr A*. Several of these stars in this so-called SgrA* cluster show proper motions in excess of 1000 km s^{-1} (see figure 3). The analysis shows that the projected velocity dispersion of stars increases towards the center as expected in the potential of a large central point mass (a 'Kepler law'). The location of the largest stellar velocities (the dynamic center), the stellar density maximum and the position of SgrA* all agree to within ±0.004 pc. The final distribution of enclosed mass as a function of true radial separation from SgrA* is shown in figure 5 of the article on SUPERMASSIVE BLACK HOLES IN INACTIVE GALAXIES. Simple physical considerations show that this central object with such a high mass and density cannot be stable and must be present in the form of a supermassive black hole. Together with the nucleus of NGC4258 (Greenhill *et al* 1995, Myoshi *et al* 1995)—in which very long baseline radio interferometric observations discovered a rapidly rotation circumnuclear disk—the galactic center currently is the very best case for a supermassive black hole.

Ultraluminous infrared galaxies

The extragalactic infrared background radiation and the identification of individual FIR galaxies (results from COBE, ISO, SCUBA) is starting to tell the history of star formation in the early universe. The IRAS satellite discovered a class of ultraluminous infrared galaxies which have the luminosity of quasars and show obvious signs of nuclear activity and advanced tidal interactions (Sanders *et al* 1988). Ultraluminous infrared galaxies (ULIRG) represent an important stage in the evolution of a wide variety of extragalactic objects including powerful nuclear starbursts, radio galaxies and quasars. They may also represent a primary stage in the formation of elliptical galaxy cores via the merger of two gas-rich spirals. ISO could contribute significantly to the investigation of ULIRGs. The ISO SWS and ISOPHOT mid-infrared spectroscopic survey of ULIRGs showed that 70–80% of them are predominantly powered by recently formed massive stars (Genzel *et al* 1998). However, about 20–30% are powered by a central AGN. These conclusions are based on an infrared 'diagnostic diagram' involving the ratio of high- to low-excitation mid-IR emission lines and the strength of the 7.7 μm PAH (polycyclic aromatic hydrocarbon) feature. At least half of the sources probably have simultaneously an active nucleus and recent or on-going starburst activity in a 1–2 kpc diameter circumnuclear disk or ring. No obvious trend for the AGN component to dominate the most compact, and thus most advanced, mergers was found. Instead, at any given time during the merger evolution, the time-dependent compression of the circumnuclear interstellar gas, the accretion rate onto the central black hole and the associated radiation efficiency may determine whether star formation or AGN activity dominates the luminosity of the system.

Star formation process

The investigation of the star-formation process profits significantly from infrared and submillimeter observations (Beckwith and Sargent 1996). Although the solid particles probably make up no more than about 1% of the disk mass they produce almost 100% of the radiation between 2 μm and $\sim$1 mm wavelength. The range of strong emission from the NIR to the radio is the result of a wide variation of temperatures, from $\sim$1000 K very close to the stars to $\sim$30 K near the outer edge of the disk at several hundred AU distance from the center. This makes it relatively easy to find disks at infrared wavelengths. The silhouettes of these disks are seen by the HST against the bright background of the Orion nebula. They show flattened, elliptical shapes and demonstrate for the first time that disks are truncated sharply at their outer radii.

Disks are very common surrounding many young stars. Half of the classical T Tauri-type stars in the Taurus–Auriga and Ophiuchus dark clouds show evidence for disks. An important new finding is that disks are common in dense clusters of young stars such as at the center of the Orion nebula (Lada *et al* 1993).

In general one discriminates between four stages of star formation (Shu *et al* 1987): first dense cores form in molecular clouds while magnetic and turbulent support is lost through diffusion of neutral particles. Then a protostar with a surrounding nuclear disk is formed via a collapse of the dense cores from inside out. Following this stage a stellar wind breaks out along the rotational axis of the system and creats a bipolar outflow. Finally the infall is terminated and a young star with a circumstellar disk is revealed.

Star-forming regions

Infrared observations are especially well suited for observations of gas clouds in active star-forming regions within our own galaxy such as the Trapezium region in the Orion nebula, M17 or M49 (see e.g. Yun and Liseau 1998). The UV radiation of clusters of recently formed O- and B-stars interacts in so-called photon-dominated regions (PDR) with the surrounding dense molecular gas at a distance of only a fraction of a parsec. By heating the gas, about 0.5% of the strong UV radiation is converted into bright infrared line emission. The investigation of these lines allows us to determine the density and temperature structure as well as abundances and chemical processes in these interface regions.

The ISO SWS observations allowed detailed investigations of interstellar ices and for the first time an unbiased overview of their compositions. The results include observations of solid CO_2, solid CH_4 and HCOOH. In the gas phase important information has been obtained on the abundance of water in warm star-forming regions, through the study of rotation vibrational lines with SWS and pure rotational lines with LWS. The gas to solid state ratios are important for investigations of the gas-grain chemistry in dense clouds in star-forming regions.

Bibliography

Alloin D M and Mariotti J-M 1994 *Adaptive Optics for Astronomy* (Dordrecht: Kluwer)

Beckwith V W and Sargent A I 1996 *Nature* **383** 139

Downes D 1989 Radio Astronomy Techniques *Evolution of Galaxies—Astronomical Observations* ed I Appenzeller, H Habing and P Léna (Heidelberg: Springer)

Eckart A and Genzel R 1997 Stellar proper motions in the central 0.1 parsec of the galaxy *Mon. Not. R. Astron. Soc.* **284** 576

Genzel *et al* 1998 What powers ultra-luminous IRAS galaxies? *Astrophys. J.* **498** 579

Genzel R, Eckart A, Ott T and Eisenhauer F 1997 On the nature of the dark mass in the center of the Milky Way *Mon. Not. R. Astron. Soc.* **291** 219–34

Genzel R, Hollenbach D J and Townes C H 1994 *Rep. Prog. Phys.* **57** 417

Ghez A, Klein B, Morris M and Becklin E 1998 *Astrophys. J.* **509** 678

Kessler M F, Steinz J A, Anderegg M E *et al* 1996 *Astron. Astrophys.* **315** L27

Greenhill L *et al* 1995 *Astrophys. J.* **440** 619

Lada C J, Young E T and Greene T P 1993 *Astrophys. J.* **408** 471

Low F J and Rieke G H 1974 *Methods Exp. Phys.* **12A** 415

Myoshi M *et al* 1995 *Nature* **373** 127

Osterbrock D E *Astrophysics of Gaseous Nebulae* 1974 (San Francisco: Freeman)

Rieke G H 1994 *Detection of Light: From the Ultraviolet to the Submillimeter* (Cambridge: Cambridge University Press)

Sanders D B, Soifer B T, Elias J H, Madore B F, Matthews K, Neugebauer G and Scoville N 1988 *Astrophys. J.* **325** 74

Shu F H, Adams F C and Lizano S 1987 *Ann. Rev. Astron. Astrophys.* **25** 23

Spitzer L 1978 *Physical Processes in the Interstellar Medium* (New York: Wiley)

Tyson R K 1991 *Principles of Adaptive Optics* (Academic: San Diego)

Watt G D and Webster A S 1990 *Submillimetre Astronomy* (Dordrecht: Kluwer)

Wall J V and Boksenberg A 1990 *Modern Technology and its Influence on Astronomy* (Cambridge: Cambridge University Press)

Yun J L and Liseau R 1998 *Star Formation with the Infrared Space Observatory (ISO)* (San Fransisco: Astronomical Society of the Pacific)

Andreas Eckart